Solar wind turbulent spectrum from MHD to electron scales

O. Alexandrova[*,†], J. Saur[†], C. Lacombe[*], A. Mangeney[*], S. J. Schwartz[**], J. Mitchell[**], R. Grappin[‡] and P. Robert[§]

[*]*LESIA, Observatoire de Paris, CNRS, UPMC, Université Paris Diderot, 5 pl. J. Janssen, 92190 Meudon, France.*
[†]*Institute of Geophysics and Meteorology, University of Cologne, Albertus-Magnus-Platz 1, 50923, Cologne, Germany.*
[**]*Blackett Laboratory, Imperial College London, London SW7 2AZ, UK.*
[‡]*LUTH, Observatoire de Paris, CNRS, UPMC, Université Paris Diderot, 5 pl. J. Janssen, 92190 Meudon, France.*
[§]*LPP, 10–12 avenue de l'Europe 78140 Velizy France.*

Abstract. Turbulent spectra of magnetic fluctuations in the free solar wind are studied from MHD to electron scales using Cluster observations. We discuss in details the problem of the instrumental noise and its influence on the measurements at the electron scales. We confirm the observation of the exponential spectral shape at these scales. Analysis of seven spectra under different plasma conditions show clearly the presence of a quasi-universal power-law spectra at MHD and ion scales. However, the transition from the inertial range $\sim k^{-1.7}$ to the spectrum at ion scales $\sim k^{-2.8}$ is not universal, as we show here. Finally, we discuss the role of different kinetic plasma scales on the spectral shape, considering normalized dimensionless spectra.

Keywords: space plasma turbulence, dissipation
PACS: 52.35.Ra,94.05.-a,96.60.Vg,95.30.Qd

INTRODUCTION

Space plasmas are usually in a turbulent state, and the solar wind is one of the closest laboratories of space plasma turbulence, where in-situ measurements are possible thanks to a number of space missions [1]. It is well known that at MHD scales (frequencies below ~ 0.3 Hz, at 1 AU) the solar wind turbulent spectrum of magnetic fluctuations follows the Kolmogorov's spectrum $\sim f^{-5/3}$. However, the characteristics of turbulence in the vicinity of the kinetic plasma scales (such as the inertial lengths $\lambda_{i,e} = c/\omega_{pi,e}$, c being the speed of light and $\omega_{pi,e}$ the plasma frequencies of ions and electrons, respectively, the Larmor radii $\rho_{i,e} = V_{\perp i,e}/\omega_{ci,e}$ and the cyclotron frequencies $\omega_{ci,e} = eB/m_{i,e}$) are not well known experimentally and are a matter of debate. It was shown that at ion scales the turbulent spectrum has a break, and steepens to $\sim f^{-s}$, with a spectral index s that is clearly non-universal, taking on values in the range -4 to -2 [2, 3]. These indices were obtained from data that enabled a rather restricted range of scales above the break to be investigated, up to ~ 3 Hz. In [4] we show that at ion scales, for a wider range of frequencies (up to $10-20$ Hz), magnetic spectra measured under different plasma conditions (but always for a quasi-perpendicuar angle between the mean magnetic field **B** and solar wind velocity **V**) form a quasi-univesal power-law spectrum with $s = -2.8$. In the present paper we verify this result.

At electron scales, the observations are difficult and our knowledge is very poor. First characteristics of turbulence at such small scales were provided recently by Cluster observations in the solar wind and in the Earth's magnetosheath [5, 6, 7, 8, 4]. Solar wind observations of Sahraoui et al. [8] show that at $k\rho_e \simeq k\lambda_i = 1$ there is a second spectral break with a new power-law $\sim f^{-4}$ at smaller scales. Solar wind observations of Alexandrova et al. [4] show that just below the electron scales the spectrum starts follow an exponential and at scales $k\rho_e \sim k\lambda_i > 1$ the spectrum deviates from the exponential and follows a new power-law, in agreement with [8], but it is an effect of the instrumental noise. Here we confirm our observations.

In the last section of the present paper, we consider normalized dimensionless spectra and we discuss the role of different kinetic plasma scales.

TURBULENT SPECTRUM AT ELECTRON SCALES

In solar wind plasma at 1 AU, electron scales are usually of the order of a few km and in the frequency spectra we find them around $100-300$ Hz. STAFF instrument of Cluster mission [9] can in principal cover such frequencies. However, the level of turbulence at electron scales is $\sim 10^{-6}$ nT^2/Hz and lower, that is very close to the

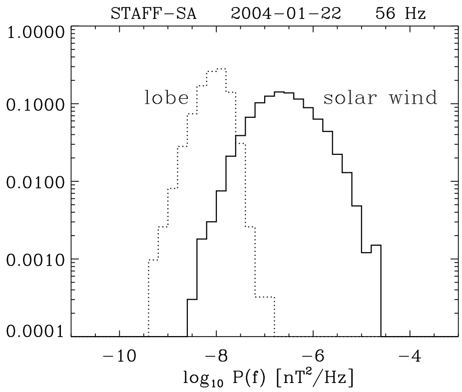

FIGURE 1. Histograms of the total PSD of magnetic fluctuations measured by STAFF-SA/Cluster instrument at $f = 56$ Hz in the lobe (left) and in the solar wind (right) during intervals of about one hour long.

instrument noise level. We will analyze in details the instrumental noise and its influence on the turbulent spectrum.

In our analysis we use measurements of STAFF-Spectral Analyzer (SA). This instrument provides four seconds averages of the power spectral density (PSD) of the magnetic fluctuations at 27 logarithmically spaced frequencies, between 8 Hz and 4 kHz.

To estimate the noise of STAFF-SA instrument, we use measurements in the magnetospheric lobes. In this region plasma activity is negligible and the instrument measures its noise only. We use lobe data on 5 April 2001, during the [6:00-7:00]UT time period. Left histogram of Figure 1 shows the distribution $H(p_{lobe})$ of the total power spectral density in the lobe, p_{lobe}, at a fixed frequency, 56 Hz. The center of $H(p_{lobe})$ is around 10^{-8}nT^2/Hz. At others 26 frequencies of STAFF-SA we observe similar histograms, but with different central PSD. Right histogram shows the distribution $H(p_{sw})$ of the same quantity but measured during one hour in the free solar wind with rather important level of turbulence. We can see that this last histogram is centered around $5 \cdot 10^{-7}$nT^2/Hz and that there is an intersection with the lobe histogram. So, even if the expectation value $\langle P_{sw} \rangle = \int p_{sw} H(p_{sw}) dp_{sw}$ of the solar wind distribution is much higher than the one of the lobe distribution, the mean true solar wind turbulence energy can be affected. Let's check how.

Distribution $H(p_{sw})$, measured by STAFF-SA at a fixed frequency, is a superposition of the turbulent signal distribution $H(p_{turb})$ and the noise one $H(p_{lobe})$. It is well known, that an expectation value of the sum of two random variables, independent or not, is the sum of expectation values of these variables. Therefore, the mean PSD of the turbulent signal at each frequency can be determined as the difference between the corresponding expectation values

$$\langle P_{turb} \rangle = \langle P_{sw} \rangle - \langle P_{noise} \rangle .$$

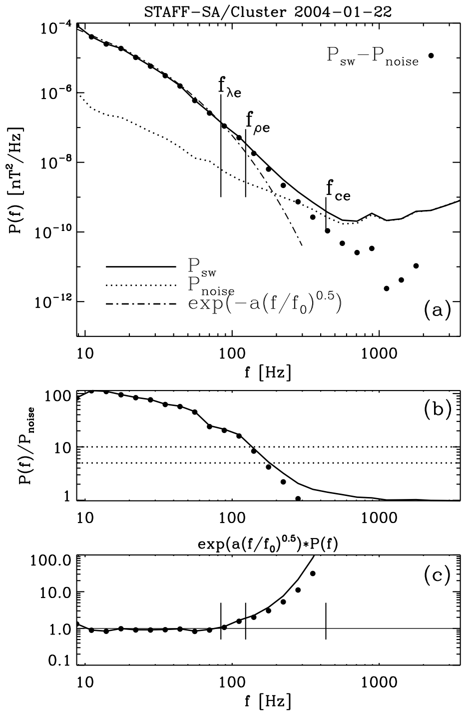

FIGURE 2. (a) Solid line shows the turbulent spectrum in the solar wind measured by STAFF–SA/Cluster instrument on 22 January 2004, 05:03-05:45UT. Dotted line shows the instrumental noise level. Black dots show the corrected spectrum. Dashed-dotted line indicates exponential fit $\sim \exp(-a(f/f_0)^{0.5})$, with $f_0 = f_{\rho_e}$ and the constant $a \simeq 9$. Vertical bars indicate electron characteristic scales. (b) Rations P_{sw}/P_{noise} (solid line) and $(P_{sw} - P_{noise})/P_{noise}$ (dots); horizontal lines indicate values of the rations 10 and 5. (c) Compensated spectrum P_{sw} by the exponential (solid line) and the corrected one (dots).

In Figure 2(a) the solid line represents the mean solar wind spectrum $\langle P_{sw} \rangle$ from 8 Hz to 4 kHz, the dotted line indicates $\langle P_{noise} \rangle$ and black dots show the resulting turbulent spectrum $\langle P_{turb} \rangle$. Panel (b) shows the rations $\langle P_{sw} \rangle / \langle P_{noise} \rangle$ (solid line) and $\langle P_{turb} \rangle / \langle P_{noise} \rangle$ (dots). From these 2 upper panel of Figure 2, one can see that for $f \geq 10^3$ Hz, the solar wind spectrum is identical with the noise spectrum, here $\langle P_{sw} \rangle / \langle P_{noise} \rangle = 1$. At $f < 10^3$ Hz, $\langle P_{sw} \rangle$ spectrum is above the noise, however, already at 140 Hz, where $\langle P_{sw} \rangle / \langle P_{noise} \rangle = 10$, is it affected by the noise, as it starts to deviate from $\langle P_{turb} \rangle$. The noise becomes very important for $f > 200$ Hz, where $\langle P_{sw} \rangle / \langle P_{noise} \rangle = 5$. So, we can not just use the measured spectrum up to the frequency where it meats the noise level, i.e. $\langle P_{sw}\rangle/\langle P_{noise}\rangle = 1$, as the solar wind turbulent spectrum, but we need to take into account the impact of the noise. The meaningful solar wind turbulence spectrum is the corrected spectrum above the noise. So, in our particular case of Figure 2, the maximal frequency is 300 Hz (where $\langle P_{turb}\rangle/\langle P_{noise}\rangle$ reach 1) and not $\sim 10^3$ Hz, as one can conclude using $\langle P_{sw}\rangle$ spectrum only.

Now, let us focus on the spectral shape. Dashed-doted line in Figure 2(a) gives an exponential fit $\sim \exp(-a(f/f_0)^{0.5})$. This is the best fit with $\langle P_{sw}\rangle$ and $\langle P_{turb}\rangle$ in the frequency range up to 100 Hz, where the noise doesn't affect the observed spectrum and both spectra are identical. At $f > 100$ Hz, that corresponds to the scales smaller than the electron inertial and electron Larmor radius (Doppler shifted scales are indicated in the spectrum correspondingly $f_{\lambda_i} = V/2\pi\lambda_i$ and $f_{\rho_i} = V/2\pi\rho_i$), the spectra $\langle P_{turb}\rangle$ and $\langle P_{sw}\rangle$ follows different power-laws. However, the presence of the close noise prevents us to conclude anything about the spectral shape at this frequency range. Figure 2(c) shows compensated spectra $\sim \exp(a(f/f_0)^{0.5})P(f)$ with $P(f) = \langle P_{sw}\rangle$ (solid line) and $P(f) = \langle P_{turb}\rangle$ (black dots). One can see that both spectra are indeed very flat up to f_{λ_e}. This confirms the exponential fit up to 100 Hz shown in Figure 2(a) and our results presented in [4].

SPECTRUM FROM MHD TO ELECTRON SCALES

Now, let us consider the combination of STAFF-SA spectrum with the spectra measured by FGM [10] and STAFF-SC [9] instruments at lower frequencies. We have analyzed such combined spectra in [4]. It was shown that for a quasi-perpendicular configuration between the mean solar wind velocity **V** and the magnetic field **B**, under different plasma conditions magnetic spectra show a quasi-universal form: $\sim f^{-5/3}$–power law at MHD scales ($f < 0.3$ Hz), at ion scales, between 1 and 10 Hz it follows a $f^{-2.8}$–power law and at higher frequencies – an exponential as we confirm here with Figure 2.

This quasi-universal spectrum was obtained by a superposition of seven spectra using (i) the Taylor hypothesis $k = 2\pi f/V$, $P(k) = P(f)V/2\pi$ and (ii) an intensity factor $Q_0(j) = \langle P_j(k)/P_1(k)\rangle$, where $P_1(k)$ is a reference spectrum and $\langle\cdot\rangle$ is a mean over the range of wave vectors covering MHD and ion scales. Let us now superpose the spectra independently at MHD scales and at ion scales. For this we define two different factors, Q_1 and Q_2. Q_1 is determined in an interval of the inertial range $[0.5, 2]\cdot 10^{-3}$ km^{-1} indicated by vertical dashed lines in Figure 3(a). One can see, that here the spectra form one clear spectrum following the $k^{-1.7}$–power law. At higher k, the spectra spread just above the break point, up to $k \simeq 0.04$ km^{-1}, and then appear to be parallel to each other. Q_2 is determined at ion scales, in the interval $[0.04, 0.1]$ km^{-1}, see vertical dashed lines in Figure 3(b). One can see that the seven spectra are superposed perfectly in this range and form a clear $\sim k^{-2.8}$–power law. Note, that this $k^{-2.8}$–range does not start exactly above the break scale, but only above $k_{\lambda_i} = 1/\lambda_i$ and $k_{\rho_i} = 1/\rho_i$.

Our results seem to be inconsistent with [3], where a variation of the spectral index between -4 and -2 beyond the first spectral break was observed. Indeed, as we have already mentioned, these observations have been done up to ~ 3 Hz only (that is of the order of $4\cdot 10^{-2}$ km^{-1}), where we observe dispersed spectra as well, see Figure 3. The spectrum $\sim k^{-2.8}$, starts for frequencies significantly higher than that of the first break. This signifies that the transition from $k^{-1.7}$ inertial range to $k^{-2.8}$ range is not universal, but depends on plasma

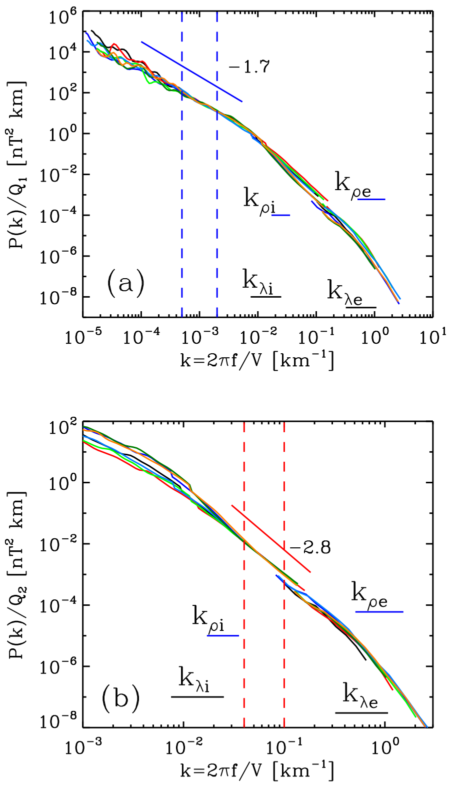

FIGURE 3. (a) Spectra for 7 time periods in the solar wind, studied in [4], rescaled by Q_1; (b) The same spectra as in (a), but for $10^{-3} < k < 3$ km^{-1}, rescaled by Q_2. Vertical dashed-dotted lines indicate wave vector ranges where Q_1 and Q_2 were determined; solid lines refer to the power laws $k^{-1.7}$ and $k^{-2.8}$; horizontal bars indicate plasma characteristic scales. Color code corresponds to different time periods, listed in [4].

conditions. This dependence can be find from the analysis of the differences between factors Q_1 and Q_2. The factor Q_1 correlates with ρ_e and with B, as was observed for the factor Q_0 [4]. Q_2 correlates best with ρ_e and to a lesser extend with B. We did not find any clear dependence for Q_1/Q_0. For Q_2/Q_0 there is a tendency of a dependence on β_e, but with the seven time periods analyzed here it is difficult to make any conclusion. More statistics are needed.

DIMENSIONLESS SPECTRA

It is interesting to compare turbulent spectra under different plasma conditions not only at the same wavevectors k in km^{-1}, as we did in the previous section, but at the same k or f measured in the characteristic scales of plasma, such as $\rho_{i,e}$, $\lambda_{i,e}$ and $f_{ci,e}$. If r is a characteristic plasma scale, normalization of k on r apply the corrections of the observed spectra accordingly:

$$P(kr) = P(f)\frac{V}{2\pi r}.$$

Such spectra have the dimension of nT^2. Normalization over B^2 yields to dimensionless spectra presented in Figure 4. Here panel (a) shows the normalized spectra as a function of $k\rho_i$, (b) $k\lambda_i$, (c) $k\rho_e$ and f/f_{ci}.

An advantage of this representation is that such turbulent spectra in the solar wind can be directly compared with any magnetic spectrum of different astrophysical or plasma device turbulent systems and without any assumptions on turbulent models.

It is a long standing problem to distinguish between different plasma scales: which of them is responsible for the spectral break at ion scales and which of them plays the role of the dissipation scale in space plasmas. From Figure 4(a) and (b) it is still difficult to say which of the ion scales is responsible for the spectral break: the break is observed exactly between $k\rho_i = 1$ and $k\lambda_i = 1$. It is possible that both scales are crucial for the change of turbulence nature at the limit of the MHD description.

Now, let us consider $k\rho_e$–normalization, Figure 4(c). It is interesting, that all the spectra are nearly collapse at scales smaller than the spectral break at ion scales. This distinguish electron gyro-radius from the other spacial plasma scales. Similar, but less clear collapse is observed in panel (d), where the spectra $P(f/f_{ci})/B^2$ are shown. These observations confirm our results presented in [4].

CONCLUSIONS

In this paper we have analyzed in details the problem of the noise of the STAFF-SA instrument and its impact

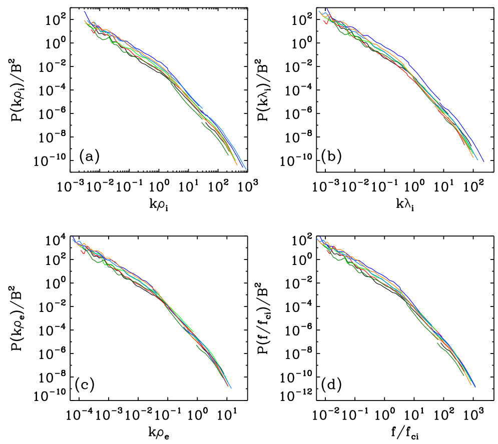

FIGURE 4. Normalized dimensionless spectra as a function of (a) $k\rho_i$, (b) $k\lambda_i$, (c) $k\rho_e$ and (d) f/f_{ci}.

on the measurements of the spectral energy in the solar wind. The noise was determined from the magnetospheric lobe measurements in the absence of any plasma activity. We show that the impact of the noise starts already when the measured spectrum is 10 times higher than the noise, $P_{sw}/P_{noise} = 10$. The impact becomes very important for $P_{sw}/P_{noise} \leq 5$. Therefore, one can not use the measured spectra until the frequency where it meats the noise level, but only until $P_{sw}/P_{noise} = 5-10$. At higher frequencies, the meaningful spectrum is the corrected spectrum above the noise level.

In the rest of the paper we have confirmed our results presented in [4]. Finally, we have discussed the role of different kinetic plasma scales on the spectral shape, considering normalized dimensionless spectra.

REFERENCES

1. R. Bruno, and V. Carbone, *Living Rev. in Sol. Phys.* **2**, 4 (2005).
2. R. J. Leamon, *et al.*, *J. Geophys. Res.* **103**, 4775 (1998).
3. C. W. Smith, *et al.*, *Astrophys. J.* **645**, L85 (2006).
4. O. Alexandrova, *et al.*, *Phys. Rev. Lett.* **in press** (2009), `arXiv:0906.3236`.
5. A. Mangeney, *et al.*, *Ann. Geophys.* **24**, 3507–3521 (2006).
6. C. Lacombe, *et al.*, *Ann. Geophys.* **24**, 3523–3531 (2006).
7. O. Alexandrova, *et al.*, *Ann. Geophys.* **26**, 3585 (2008), `arXiv:0810.0675`.
8. F. Sahraoui, *et al.*, *Phys. Rev. Lett.* **102**, 231102 (2009).
9. N. Cornilleau-Wehrlin, *et al.*, *Ann. Geophys.* **21**, 437 (2003).
10. A. Balogh, *et al.*, *Ann. Geophys.* **19**, 1207 (2001).